3-D microscope using diffraction grating

Tom DeWitt
DeWitt Brothers Tool Company, Inc.
237 Lafayette St., New York, NY 10012

Douglas Lyon
University of Bridgeport, Computer Science and Engineering Department
Bridgeport, CT 06460
***E-mail*: Lyon@cse.bridgeport.edu**

Abstract

An optical microscope has been adapted for 3-D inspection of small capillaries in thread spinnerets by placing a diffraction grating between the microscope objective and the specimen. We show how a grating was specified using a quantitative analysis of groove spacing and geometry. An illumination system was specified based on incident angle and light wavelength. Specimens are placed on a robotic stage for positioning, and repositioning affords multiple perspective views of the target depending upon the diffraction order visible to the objective.

Keywords: diffraction, range finder, microscope, grating, 3-D, third-dimension, profilomery, machine vision, metrology

1. Hole Metrology

We have previously demonstrated the diffraction range finding technique for depth measurements on convex or moderately concave surfaces [1-10]. An extreme case of concave geometry are cavities with parallel walls, i.e., holes. While commonplace in manufactured products, there are no ubiquitious optical instruments for their inspection.

A key parameter in designing a hole metrology system is occlusion immunity, that is, the capability of the sysem to overcome shadowing effect caused by the hole walls. Occlusion particularly affects triangulation systems, because their readings are based on the baseline separation between a transmitter and a receiver. Decreasing a triangulation baseline will improve the system's occlusion immunity but at the expense of range resolution. We compare a triangulation set-up with our diffraction method in Figure 1 on the following page. The occlusion liability is inscribed as angle ß, and can be determined for a triangulation system by measurement of the hole diameter d_h and the hole length L .In a practical device, we may wish to use a value of 1/2 d_h, in (1) to allow acquisition of range data from the hole floor. As illustrated in Figure 1a, where a section of the floor is blacked out, the entire floor can only be seen by a triangulation scanner if the the hole is rotated to bring the occluded section into view. Hence, for the configuration in Figure 1a, we write:

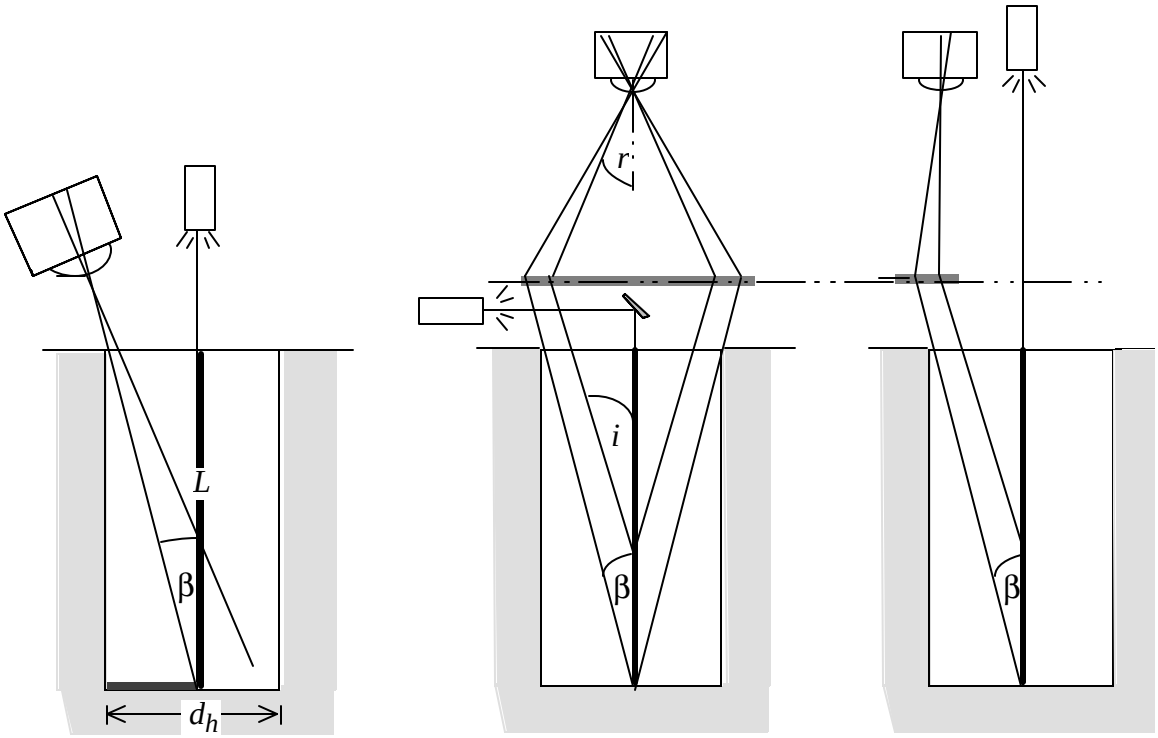

(a) Triangulation **(b) Co-axial Diffraction** **(c) Off-axis Diffraction**

Figure 1. Comparison of triangulation (a) with diffraction (b & c) hole metrology.

(1)
$$\beta = \arctan\left(\frac{d_h}{2L}\right)$$

In order to study occlusion liability in the diffraction range finding method, we invoke the Grating Equation:

(2)
$$\sin i + \sin r = \lambda\frac{n}{p}$$

where *n* = diffraction order, an integer
λ = wave length of illumination
***p* = grating pitch**
***i* = angle of diffracted ray subtended from target onto the grating**
***r* = angle of diffraction image at the receiver**

Since the angle of incidence upon the grating, *i*, will be limited to a maximum equal to the occlusion liability angle β, for any receiving angle there exists a minimum grating pitch:

(3)
$$p = \frac{n\lambda}{\sin(r) + \sin(\beta)}$$

We will show at the end of the next section how this expression can be used to specify diffraction grating pitch in specific cases.

2. Aspex SpinTrak

The reduction-to-practice of diffraction hole metrology that guided our project involved the Aspex SpinTrak™ [536 Broadway, New York, NY 10012]. The market version of this unit performs automated 2-D inspection of thread spinnerets. A schematic diagram of the apparatus appears as Figure 2 below.

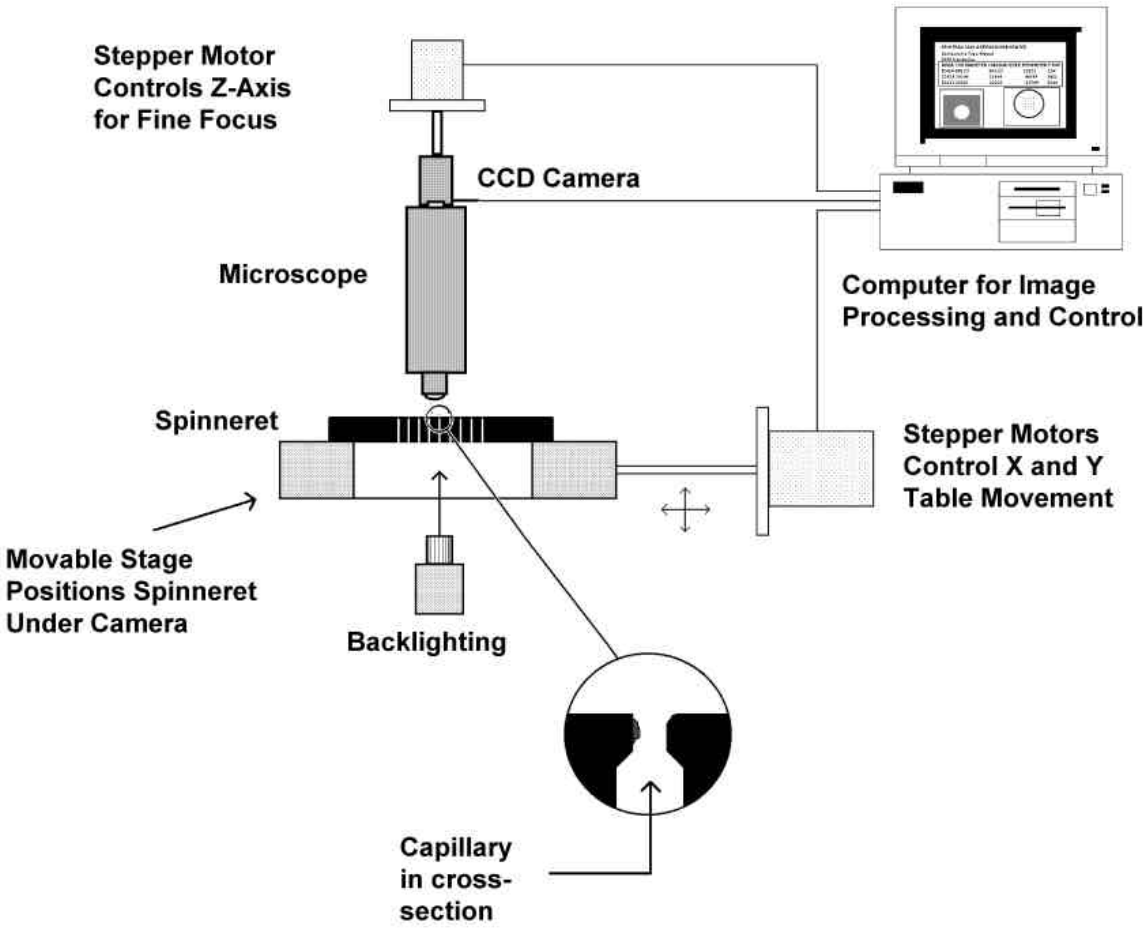

Figure 2. Schematic representation of the Aspex SpinTrak Automatic inspection CMM.

Each spinneret has dozens to thousands of tiny holes called capillaries which eject threads as part of an extrusion manufacturing process. The Aspex SpinTrak product currently on the market can detect blockages and breaches in the capillaries but cannot measure capillary depth, an important evaluation parameter requested by many users of the device. For this reason Aspex entertained our proposal to develop a 3-D metrology capability for their product.

Triangulation can be used to make measurements of capillary depth using the configuration illustrated in Figure 1(a), and as part of this research we experimented with a triangulation set-up using the Aspex microscope[11]. The experimental bench unit is illustrated in Figure 3 on the following page along with examples of an acquired image, shown in Figure 4.

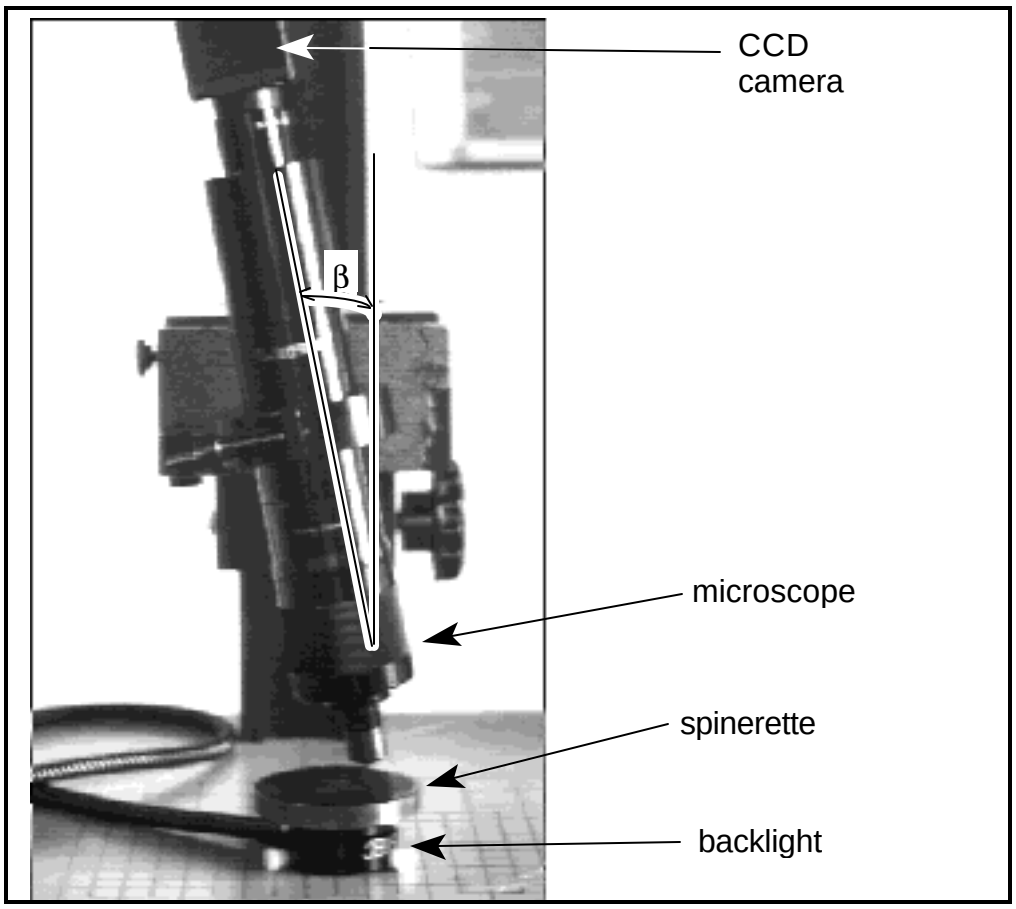

Figure 3. Experimental triangulation set-up

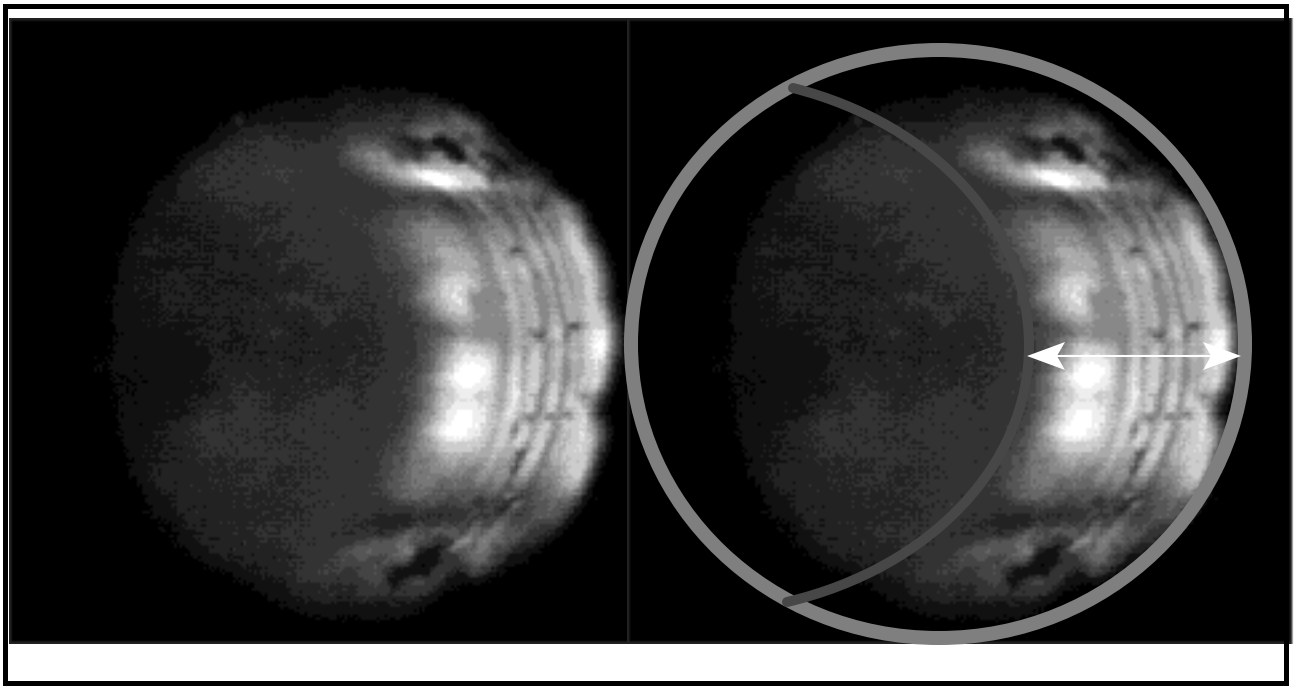

Figure 4. Triangulation view of hole. Right view diagrams method for depth measurement.

Referring to Figure 3, ß is measured at 12_. This is the rotation of the microscope which was used to capture the image shown in Figure 4. An overlay is used in the Figure 4 right hand image to indicate how hole depth could be measured. While the bottom of the hole can be distinguished clearly, short depth-of-field in the microscope obscures the lip of the hole, and this must be estimated. The hole depth is proportional to the distance indicated by the arrow.

The Aspex SpinTrak does not enjoy the option of rotating the microscope, since its 2-D metrology depends on a precise vertical alignment of the microscope. This alignment is so precise that the microscope is rigidly fixed to a bridge, and the spinnerets are moved below it on an xy table. A photograph of a typical SpinTrak unit is shown in Figure 5 below.

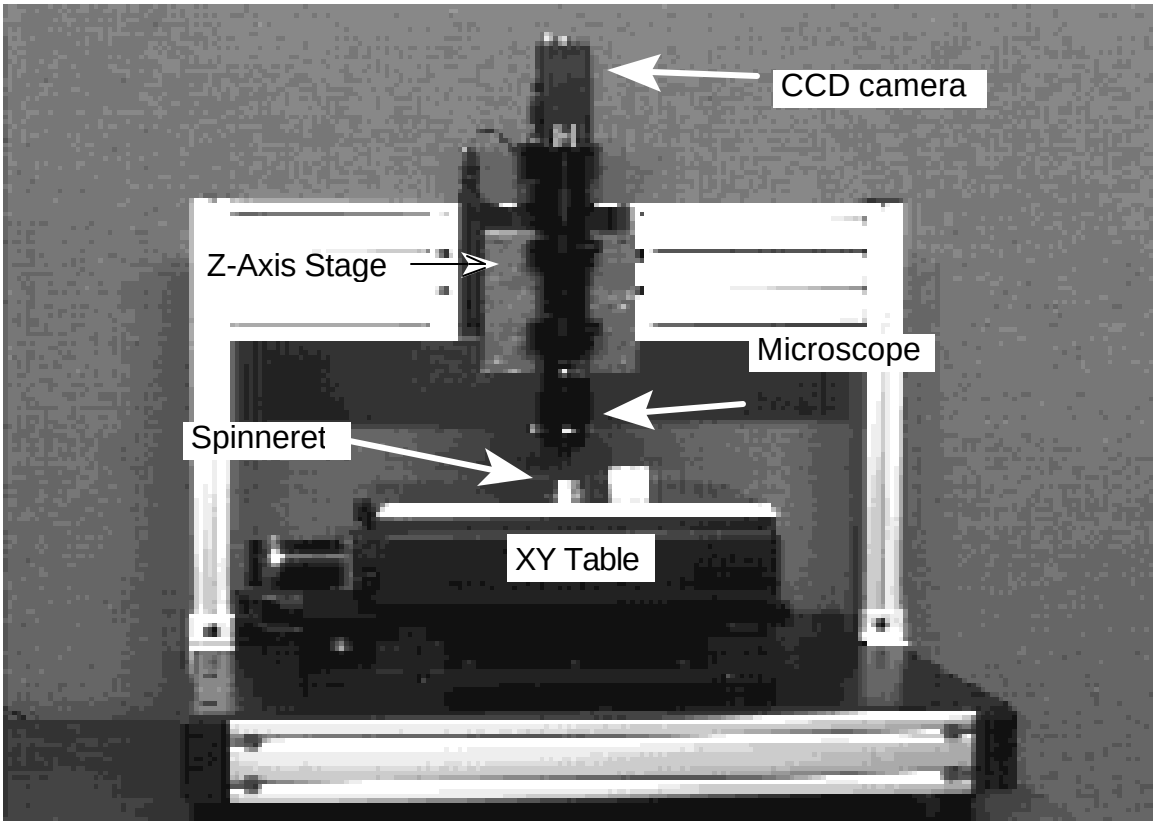

Figure 5. Aspex SpinTrak 2000

The diffraction method provides the SpinTrak with the equivalent of a rotation of the optical axis while maintaining true vertical alignment of the microscope. Moreover, the multiple spectra of diffraction in their plus and minus orders provide a plethora of views at different positions and powers of magnification.

A series of experiments were conducted using the test bed previously used for triangulation studies. However, the microscope was positioned perpendicular to the plane of the test spinneret. A grating with a pitch of 5.55 µm was placed on a glass slide above the spinneret. For rear illumination, a fiber optic ring, normally used as a front illuminator, was placed under the spinneret. This method of illumination, which was also used to produce Figure 4, provided a moderately focused beam inside the spinneret cavity leading to the capillary. Figure 6 on the next page shows the distal end of the fiber optic array.

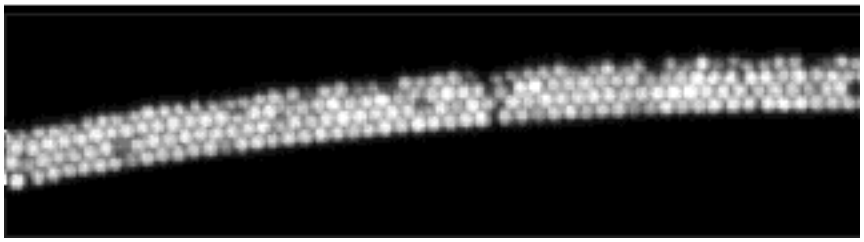

Figure 6. Fiber optic illumination bundle distal end.

The multi-spectral illumination radiating from the fiber optic light source resulted in a blurred diffraction image seen below in Figure 7

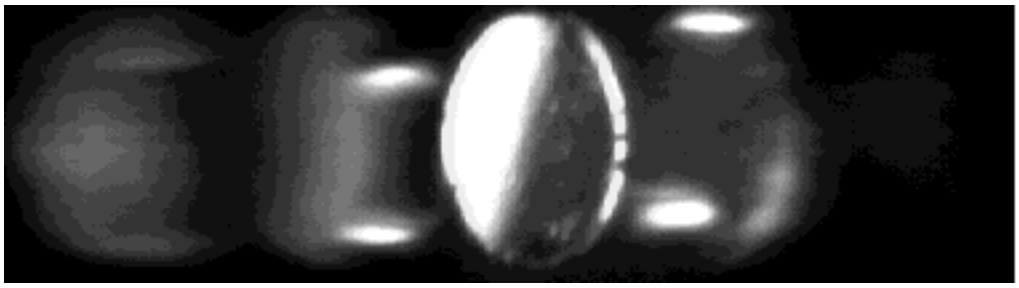

Figure 7. Diffraction image in white light illumination.

Anticipating this problem, we had obtained a laser diode with monochromatic spectral energy, nominally at 670 nm. This was used in place of the white light illumination source for the fiber optic bundle. However, the laser illumination was coherent and created a characteristic speckle pattern when imaged through the microscope as illustrated below.

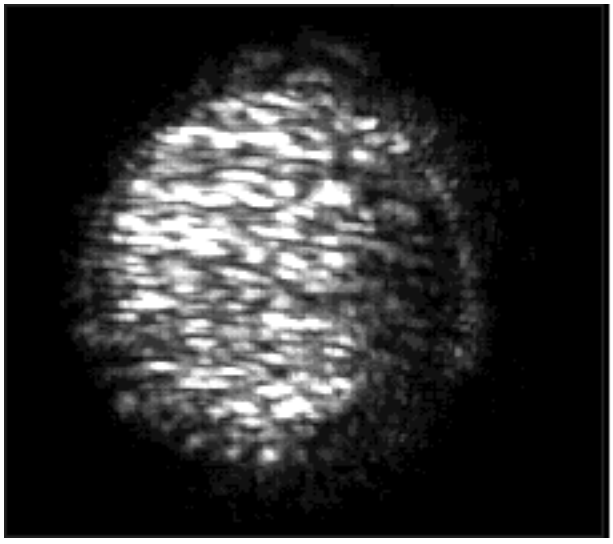

Figure 8. Laser illumination speckle. This is a zero-order image of a capillary hole.

A viable solution to the illumination problem was found by filtering the white light source with an interference filter. A 632.8 nm bandpass filter was obtained from a HeNe laser imaging lens. This was mounted inside the fiber optic illuminator housing in a line with the fiber optic bundle. The resultant image is shown on the following page as Figure 9.

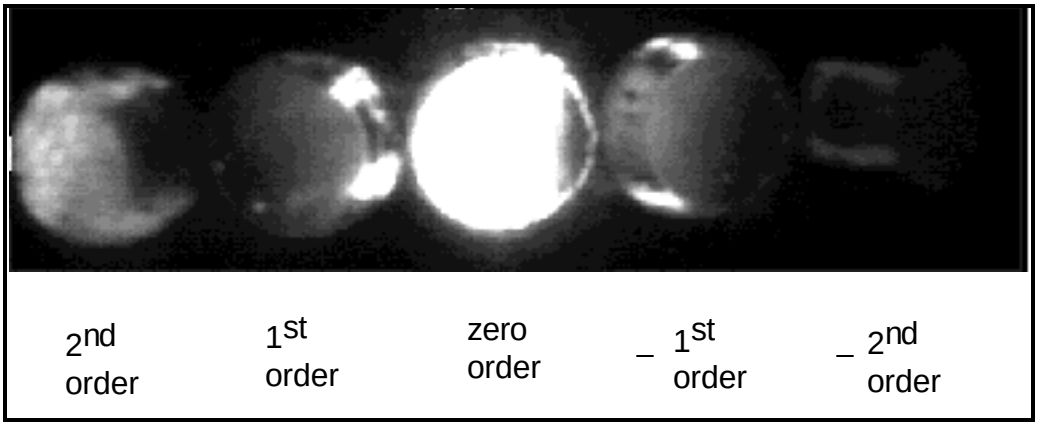

Figure 9. Diffraction image of target hole under filtered illumination.

Figure 9 shows an on-axis illumination view made with a configuration like that shown in Figure 1(b). This set-up permitted the simultaneous acquisition of four parallax views. The second order images provide greater parallax. Negative order images provide views of the hole from the opposite side of the positive orders. This is a useful feature when compared with triangulation which typically provides only a single parallax view. With diffraction, the work piece does not need to be rotated to be seen from both sides. Grating groove shape specifications can determine the selection of multiple orders – either a single higher order or many higher orders. Moreover, in addition to symmetrical plus and minus higher-order views, opposed parallax views can be generated using a cross-hatch grating, that is, a grating with orthogonally opposed rulings. An example is shown below in Figure 10.

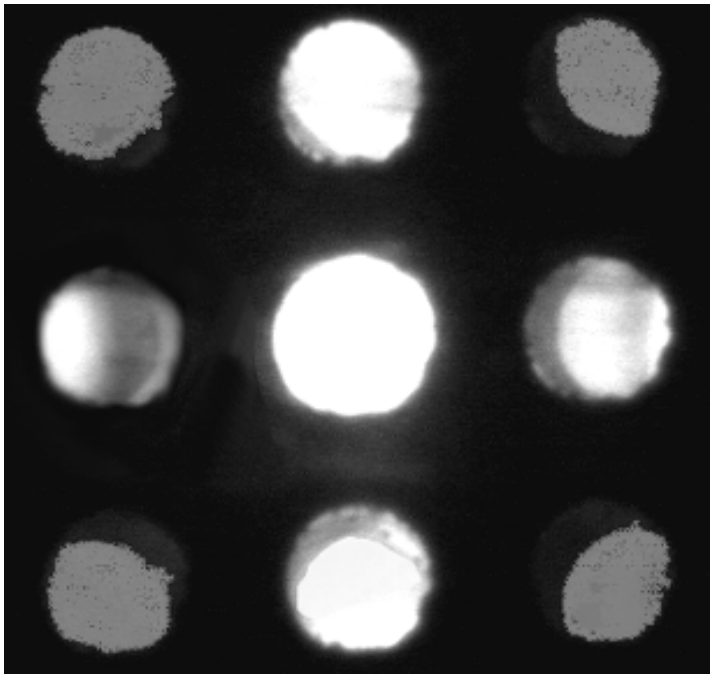

Figure 10. Two-dimensional parallax views made using a cross-hatch grating.

In order to resolve fine detail within a higher-order diffraction image, the receiver must be moved off the illumination axis. Such a configuration is illustrated in Figure 1(c). Once off the illumination axis, a diffraction image can be formed in the center of the field-of-view of

the receiver, and the receiver lens can be moved in the z-axis toward the target, allowing magnification. An example is given below in Figures 11 and 12.

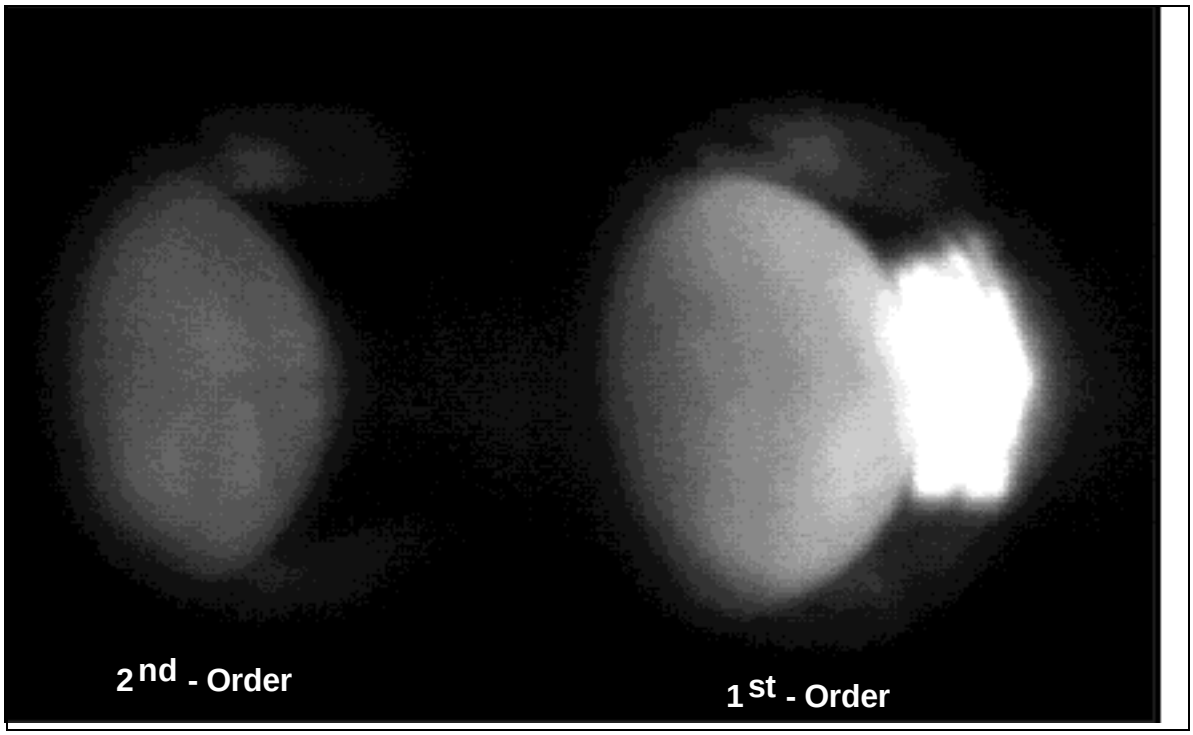

Figure 11. Magnification made possible by off-axis illumination configuration

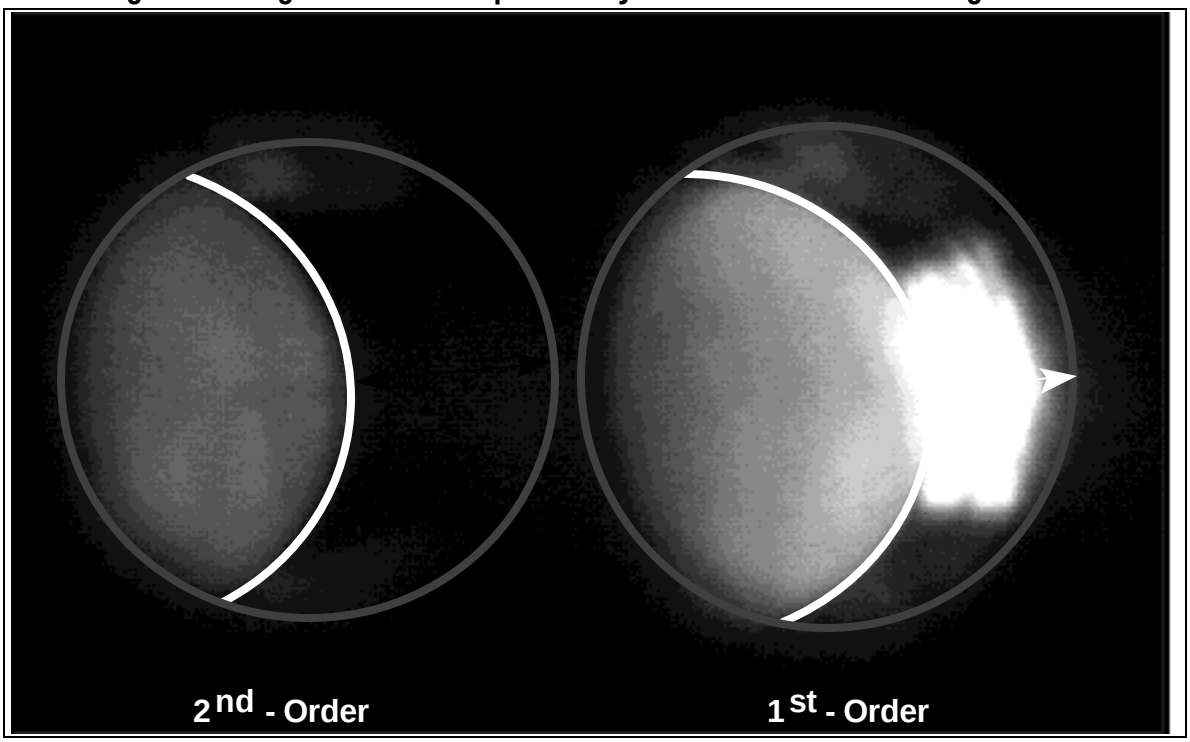

Figure 12. Determination of hole depth using detailed diffraction image

The XY translation and Z-axis zoom required to acquire the perspective views exampled in Figures 11 & 12 are completely compatible with the Aspex SpinTrak in its current form. A threaded collar that is supplied with the microscope itself can be used to hold the grating. Fiber optic illumination similar to the current modules supplied with the unit can be

upgraded to accommodate the color bandpass and focus requirements specific to the diffraction method. A schematic of a prototype instrument is illustrated in Figure 13 below.

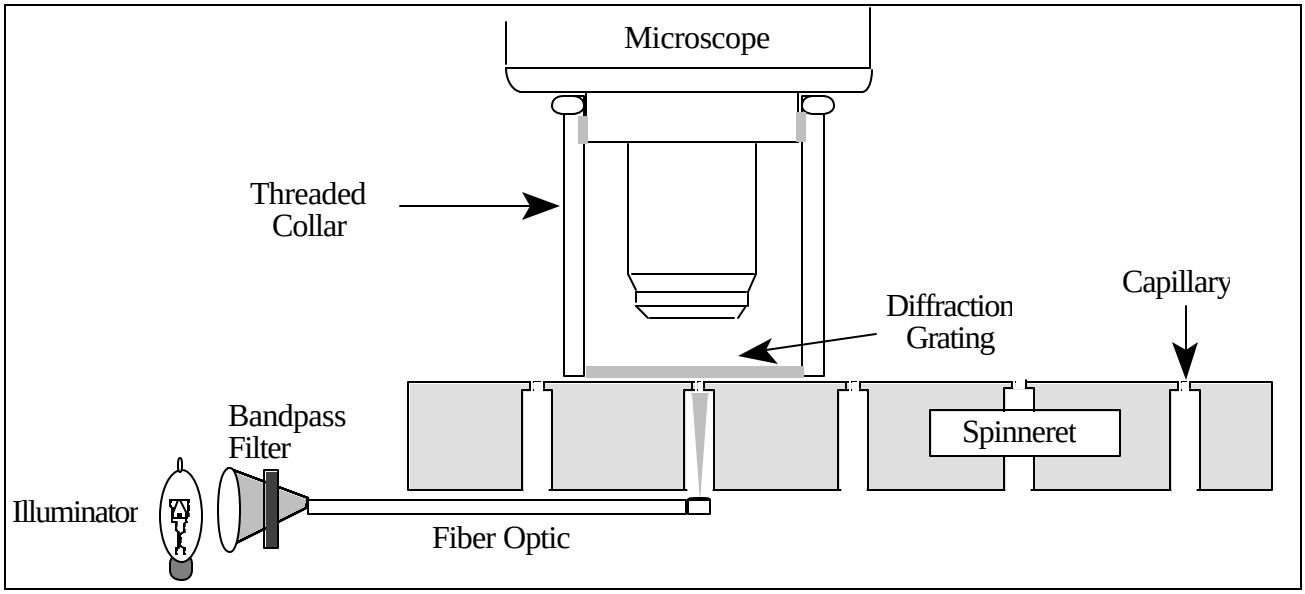

Figure 13. Diffraction range finder fitted to SpinTrak CMM

Specification of a grating pitch for the SpinTrak was guided by Equation (3). Typical spinnerets have a hole lengths L from 0.01" to 0.1" and diameters d_h from 0.01" to 0.05". Length to diameter ratios vary from 2:1 to 10:1. The microscope objective receiving angle r varies from 4_ to 7_ depending on magnification. We compare occlusion liability angles in Figure 14 below. Using Equation (3) with r set at 4_ we can specify suitable grating pitches for these occlusion conditions, as is illustrated in the matching graph.

Grating groove geometry determines the number of visible orders and their efficiency. Our experiments were conducted using embossed plastic "Spectrasheen" gratings (pitch of approximately 5 μm) available from SpectraTek of Los Angeles. These gratings produce up to three visible higher-order images. We anticipate grating fabrication by binary methods to

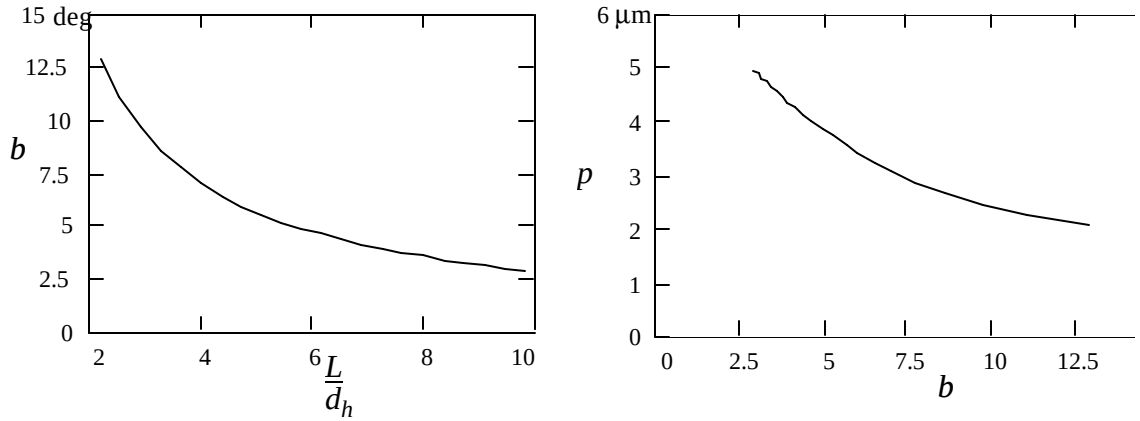

Figure 14. Left graph: Ratio of length to diameter dictates occlusion liability β. Right graph: β can be used to specify an appropriate diffraction grating pitch p.

obtain groove geometries that produce multiple orders, and we have obtained a 2.94 μm sample grating from Lasiris intended for 5 point structured illumination projection but which seems to work perfectly well as a receiver in our range finder. As our research progresses, we also expect to model the depth resolution of diffraction images as a function of the number of rulings in the active region of the grating structure. This analog to spectral resolution used to specify spectrometers is quite important in microscopy because of the small dimensions of the gratings used.

3. Other embodiments

In addition to the configuration shown in Figure 13, we have investigated refinements for microscopic examination of cavities by the diffraction method exploiting gratings which have a frequency greater than the incident illumination. This technique requires both an offset of the source illumination and a rotation of the grating.

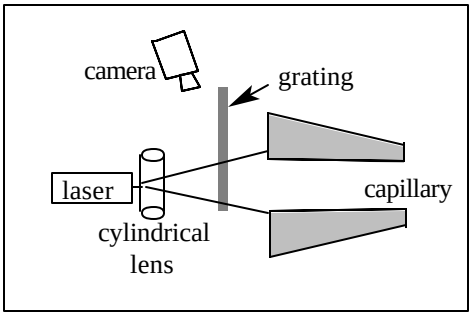

Figure 15. Possible Configuration

The possibility exists to place the illumination on the same side of the hole as the grating. The illustration, Figure 15 on the left, shows this type of geometric relationship. While this arrangement is not possible with the SpinTrak microscope, which must remain strictly vertical, we anticipated achieving equivalent geometries using relay assemblies fashioned from reflective surfaces. In this setup high frequency gratings have a potential for range magnification, and we examined them as part of our research.

Our inquiry confirmed the magnification effect we had anticipated. Using a test fixture modeled on Figure 14 we illuminated a 0.25 inch hole at various depths up to 1 inch and recorded images with a variety of macro lenses. These produced images shown on the following page in Figure 16.

The oval shaped hole lip, best seen in Figure 16 (7&8) made by "flood" illuminating a large portion of the hole lip with a defocused laser, indicates the manner by which a high frequency grating can generate increased depth resolution. Since the depth measurement is made by determining the displacement between the lip and bottom of the hole, the elongation of the lip stretches the horizontal dimension, thereby effectively increasing depth resolution of the range finder. This phenomenon, well known with anamorphic lenses and analogous to prisms [12], has not been exploited as a range finding feature and has promising potential in microscopy. However, an artifact of internal reflection within the transmission gratings used in our experiments created a series of ambiguous multiple images This is noticeable in the broadening of the laser stripe in Figure 16 (4, 5 & 6) where the stripe appears to be striated in the horizontal dimension.

A close examination of the inner reflection phenomenon is shown in Figure 17. To produce this image, the target was illuminated with a point source rather than a stripe, and the camera recorded image was enlarged. The obvious solution to the inner reflection problem with high frequency gratings is to use a reflection grating. However, the restrictions in orientation and size made this a difficult design problem not within the resources of our project.

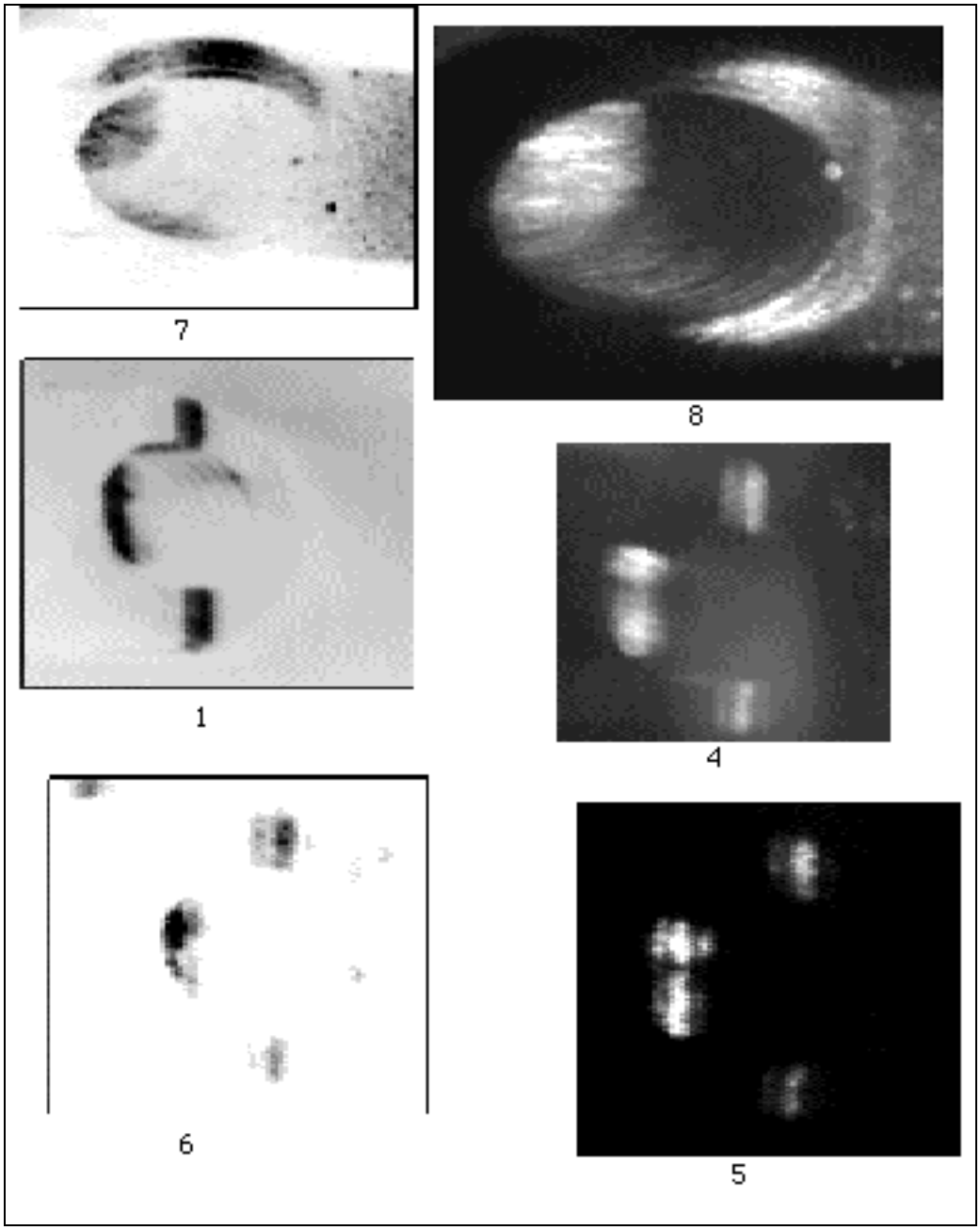

Figure 16. Examples of high frequency grating images. Negative on left; Positive on right. Top pair (7&8) illuminated by "flood" lighting. Other images illuminated by a laser stripe.

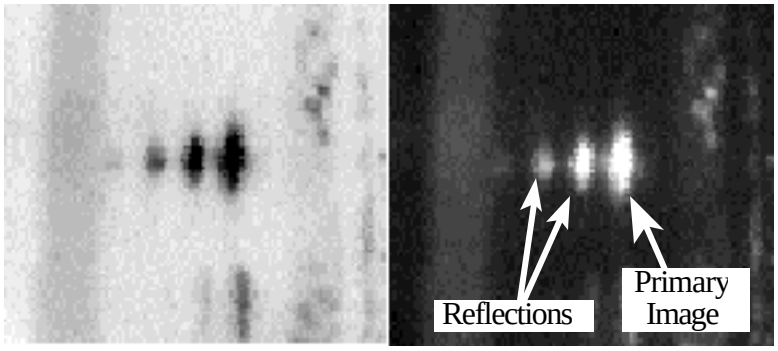

Figure 17. Inner reflections within a transmission grating. Negative and positive versions.

4. Conclusion

We have investigated a diffraction-based method for measuring depth inside of holes. We developed geometric models for occlusion immunity. Using these models and our previously published models for diffraction, we have examined a variety of configurations for diffraction range finders which are specifically optimized for metrology in occluded spaces, and we have conducted a series of experiments to corroborate predictions drawn from these models. Finally, we have attempted to adapt the diffraction method to an extant co-ordinate measurement machine built by Aspex, Inc.

5. Acknowledgements

We would like to express our appreciation for the assistance from all of the participants at Aspex, Inc. We are indebted to Bill and Julie Parker of Diffraction Ltd. [Waitsfield, VT] who provided ideas, technical advice and high frequency grating materials.

This research was supported by an SBIR grant from the New York State Science and Technology Foundation to DeWitt Brothers Tool Company, Inc. and by an Instrumentation Laboratory Improvement (ILI) grant from the National Science Foundation to the University of Bridgeport.

6. References

1. Tom DeWitt, "Novel methods for the acquisition and display of three-dimensional surfaces," *Optical and Digital Pattern Recognition,* 1987, SPIE, Vol. 754, pp. 55-63

2. Tom DeWitt, "Range Finding by Diffraction," U.S. Patent No. 4,678,324, July 7, 1987

3. Tom DeWitt, "Range Finding with Diffraction Gratings," *Advanced Imaging*, 1988, No. 12, July/August, p. A50 ff.

4. Tom DeWitt, "Diffraction Range Finding for Machine Vision," *Proceedings of Robotics 12/Vision 88,* 1988, SME, Vol 1, Section 5, pp. 139-150

6. Tom DeWitt, "Rangefinding by the Diffraction Method," *Lasers and Optronics,* 1989, Vol. 8, No. 7, April, pp. 118-124

7. Tom DeWitt, "3D Image Acquisition by Diffraction Profilometry," *Paper Summaries of SPSE's 42nd Annual Conference,* May '89, pp. 51-54

8. Tom DeWitt, "A Guide to 3-D Surface Acquisition," *Proceedings of the Tenth Symposium on Small Computers in the Arts*, SCAN 90, Nov. 1990, pp. 40-46

9. DeWitt Brothers Tool Company, "3-D Machine Vision by the Diffraction Method", NSF SBIR Proposal #III-9261621, 1992

10. Tom DeWitt. and Douglas Lyon, " Rangefinding Method Using Diffraction Gratings", *Applied Optics*, May, 10, 1995 Vol 34, No. 14, pp. 2510-2521, cf equations 7 & 8.

11. InfiniVar, Infinity Photo-Optical Company, 706 Mohawk Dr., Suite 15, Boulder, Co. 80303 tel. (303) 499-6282.

12. Rudolf Kingslake, *Optical System Design*, Academic Press, p. 308 *ff.*